Fracture Simulation for Deep Crystalline Rock

Chaoshui Xu[1] and Peter A. Dowd[2]*
[1] School of Civil, Environmental and Mining Engineering, University of Adelaide
[2] Faculty of Engineering, Computer and Mathematical Science, University of Adelaide
* Corresponding author: Peter.Dowd@Adelaide.edu.au

This paper describes the application of simulated annealing for fracture modelling in crystalline rock. The technique is capable of incorporating the spatial correlations of fracture properties within a fracture set or across different fracture sets so that more realistic fracture systems can be simulated.

Keywords: marked point process, discrete fracture network, *K*-function, simulated annealing

Introduction

Realistic fracture models are crucial for the design and performance assessment of geothermal reservoirs, especially in hot dry rock (HDR) applications. The model is the fundamental input required for the modelling of fluid flow through the 3D fracture network comprising initial fractures and new fractures created by hydraulic stimulation. The characterisation of rock fracture networks is an extremely difficult problem not least because accurate field measurement of a single discontinuity is difficult and measurement of all discontinuities is impossible. For these reasons, in practical applications, there is no observable reality of the 3D network on any meaningful scale and the only realistic approach is via a stochastic model informed by sparse data and/or by analogues.

The first step in stochastic fracture modelling is data collection and statistical analysis, from which model parameters are derived. Data normally come from surveys of analogues, such as rock outcrops, or from direct or indirect observations of the rock mass such as drill cores, borehole imaging, geophysical surveys or seismic monitoring during fracture stimulation. In general, the outcomes of this step include the identification of fracture sets, the distribution characteristics of fracture locations, and statistical distributions of fracture properties, such as orientation, size and aperture. On the basis of these parameters it is then possible to generate a 3D fracture network for the reservoir, which is a possible "reality" in the sense that all statistical characteristics of the network are reproduced.

The two most commonly used mathematical methods for stochastic fracture simulation are Poisson planes (Dershowitz and Einstein, 1988) and random object models (Stoyan et al., 1995, Molchanov, 1997), with the latter more popular because of its flexibility for adaption to a wide range of applications. Current practice in random object models is to generate fractures via a Boolean-type approach (Stoyan et al. 1995, Molchanov 1997, Chilès and Delfiner 1999). The fractures are divided into sets and parameters for location, size and orientation are modelled separately for each set. The final fracture model is the combination of each set of fractures generated independently. Spatial correlation is considered only for modelling the fracture intensity which defines the number of fractures in a particular area (2D) or volume (3D). Other spatial correlations, either auto-correlation for an individual variable or cross-correlations between pairs of variables, within a fracture set or between different fracture sets, are generally ignored. These correlations, however, must be included to generate realistic fracture models.

Boolean object model

It is common practice to classify observed fractures (traces) into sets according to their orientations and to study each set independently. The separation of fractures into different sets is based on the belief that fractures formed by tectonic activity are likely to be oriented in approximately the same direction and to display similar properties (e.g., size, aperture). It is therefore reasonable to study the sets individually.

The generation of a Boolean object model is relatively straight-forward (Xu and Dowd, 2009). For a given fracture set, the fracture locations are generated first, usually by a Poisson distribution in which fracture intensity for a particular area (2D) or volume (3D) is either assumed to be constant or is derived from geostatistical estimation or simulation. Secondly, the orientation of each fracture is generated, most commonly from a Fisher distribution. Finally, the size of each fracture is generated from a specified distribution, the most common being exponential, lognormal or gamma. Other fracture properties, such as aperture and joint strength, can then be added into the network by additional Monte Carlo steps. Options for fracture intersections and termination/truncation can also be incorporated. Additional fracture sets can be generated in a similar fashion (independent simulation) to produce the final fracture model.

A common approach to the statistical analysis of fracture models is to use marked point processes. Fracture locations are represented by points (centre point or a random point on the fracture) in space and all fracture properties, such as orientation, size and aperture, are represented by marks associated with the points. In this context a Boolean object model can be described as a

realisation of a point process with independent markings. A two-dimensional example is given in Figure 1, which shows fracture traces on a Yucca Mountain outcrop, as mapped by Barton and Larson (1985). Similarly, three-dimensional representations of fractures by marked points can also be constructed provided the shapes of the fractures are assumed.

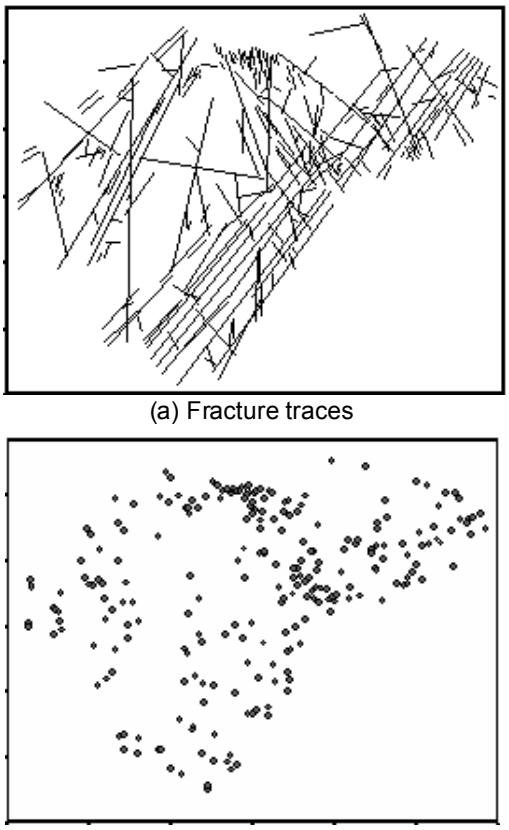

(a) Fracture traces

(b) Point representation

Figure 1 Two-dimensional fracture pattern and the corresponding point representation, Barton and Larson (1985)

This simplistic fracture model assumes no spatial correlation among the fracture sets, and no spatial correlation between fracture properties and fracture locations and among fracture properties themselves. The only spatial correlation model included in the model is the fracture point density defined as the number of fracture representation points per unit area (2D) or per unit volume (3D). This correlation is imposed either by using a geostatistical model to simulate the fracture point density or implicitly by various types of point patterns (homogeneous, non-homogeneous, cluster or Cox point process).

Spatial correlations in fracture modelling

In general, fractures sets tend to be correlated (Chilès and Marsily, 1993). This is supported by the observation that different fracture sets may be formed by different tectonic events active at different times, which raises the possibility that the formation of newer fractures is likely to be influenced by existing fracture networks. The extent and significance of the correlations can vary but can cover various aspects of the fracture properties. For example, five fractures sets are identified for the fracture pattern in Figure 1a; the auto- and cross- ***K***-functions of the fracture locations shown in Figure 2a and b (Xu and Dowd, 2008) show that the fracture locations of different fracture sets have some association and are not independent. Either a hierarchical model (Lee et al. 1990) or plurigaussian simulation (Dowd et al. 2007, Xu & Dowd 2008) can be used to incorporate these correlations into the fracture model. A cluster point process is another type of model that can takes the correlation of fracture locations into account during fracture model construction.

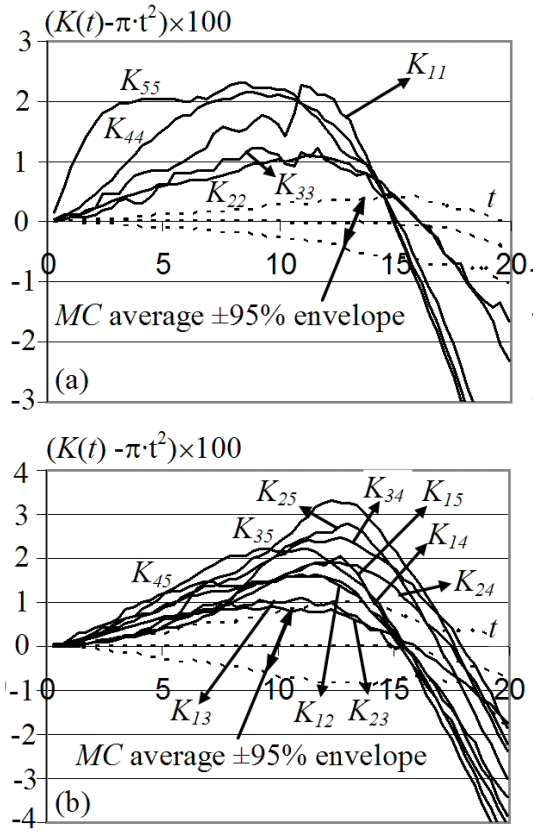

Figure 2 Auto- and cross- ***K***-functions for the point dataset Figure 1b

Fracture properties can also be correlated and the correlation can be among fractures in the same set or across different sets. These correlations are ignored in the Boolean object model, i.e., marks generated in the model are spatially independent. Practical observation and statistics (Priest 1993, Lee and Farmer 1993, Baghbanan and Jing 2007, Chilès and de Marsily, 1993) suggest high correlation between fracture size and aperture. Sizes and locations of fractures are always spatially correlated, even if the fractures belong to the same fracture set. The general practice of classifying fractures in sets and their

independent treatment is an indication that fracture properties are highly correlated with orientation. For realistic fracture modelling these correlations cannot be ignored.

Demonstration of the incorporation of correlations in fracture model

Figure 3a shows a simulated 3D fracture system generated in a volume of interest of size 100×100×100. In reality, such an image is difficult to obtain and we are restricted to the use of exposed 2D images such as rock outcrops or quarry faces. An example of this type of image is shown in Figure 3b, which was obtained by cutting Figure 3a by a north-south vertical cross-sectional plane (shown), thus simulating an exposed quarry face. The fracture trace lines on the image can now be analysed to construct a possible model to describe the pattern. Using the mid-points of the trace lines, the corresponding point dataset for the fractures is shown in Figure 3c.

We consider here two marks for each point, the fracture trace length, ξ, and orientation α. Angle α is measured clockwise from the vertical direction and it is, therefore, necessary to make the transform to $\beta = |\alpha - \pi/2|$ $(0 \le \beta \le \pi/2)$ for the convenience of analysis. After this transformation, small β values correspond to near horizontal lines (parallel to Northing direction in Figure 3a) and large β values suggest the lines are nearly vertical (parallel to vertical direction in the Figure 3a).
The correlation coefficient between ξ and β is estimated as 0.48 and the distributions of ξ and β are estimated using a kernel density estimate which show lognormal and uniform types respectively. We fit an approximate lognormal distribution with a mean of 0.8 and a variance of 2.0 in logarithmic scale for ξ. The positive correlation between β and ξ indicates that the two marks are highly correlated, i.e., vertical fractures tend to be longer than horizontal ones. In summary, for the example,

1. ξ follows a lognormal distribution (with estimated mean of 0.8 and variance of 2.0 in logarithmic scale).
2. α and β follow a uniform distribution on the interval [0, π].
3. ξ and β are positively correlated with correlation coefficient 0.48, i.e., in physical terms vertical fractures tend to be longer.

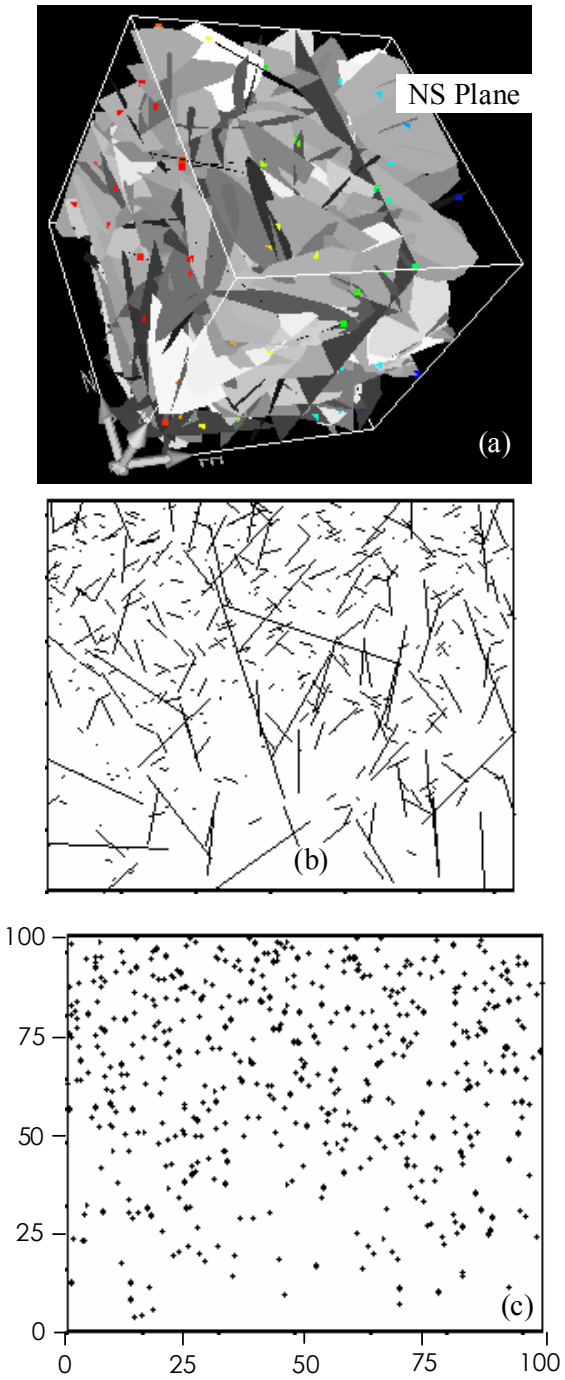

Figure 3 Simulated example: (a) 3D fractures, (b) Fracture traces on the plane, (c) Representing point pattern

To quantify the spatial correlations between ξ and β, we use the cumulative spatial mark correlation function introduced by Xu et al. (2007):

$$K_m(t) = \frac{1}{K(t)\bar{f}_m}\frac{gw_g}{\lambda^2}\int_0^t u^{g-1}\lambda_2^{(f)}(u)du$$

where $w_g = \sqrt{\pi^g}/\Gamma(1+g/2)$ is the volume of the unit ball in $\Re^g$, $K(t)$ is the second order ***K***-function, λ is the point density, $\lambda_2^{(f)}$ is the second order *f*-product density function for the point field and f in this definition is the application-dependent mark function. Based on this

definition, $K_m(t) \equiv 1$ if there is no correlation between marks at distance t.

For the example (Figure 3), Figure 4a shows the spatial auto-mark correlation function for fracture line length ξ and Figure 4b shows the spatial auto-mark correlation for fracture orientation β. The spatial cross-mark correlation function between ξ and β is given in Figure 4c. The Monte Carlo (MC) simulation envelope (average value and ±95% bounds) for the case of spatially uncorrelated marks is also plotted on the graphs. These three figures reveal some important spatial characteristics between the marks in the simulated example dataset; briefly:

4. Smaller values of $\hat{K}_{\xi}(t)$ for small t indicate that fractures (points) close to each other tend to be shorter (smaller mark ξ). In physical terms, aggregated fractures tend to be shorter in length. Although this feature is not apparent in Figure 3b, it is widely observed in practice that short fractures in rock tend to occur in clusters as the result of local thermal effects and long fractures caused by geological movement (forces) tend to be more isolated or sparsely distributed.
5. Smaller values of $\hat{K}_{\xi\beta}(t)$ for small t suggest that fractures (points) close to each other tend to be horizontal and shorter. In physical terms, aggregated fractures in this particular dataset are more horizontally oriented and longer fractures tend to be more vertically oriented and more sparsely distributed.
6. The flat appearance of $\hat{K}_{\beta}(t)$ suggests that, in terms of fracture orientation, there is no preferential direction of the pattern of fracture aggregation.

The aim of simulating a fracture set that resembles Figure 3b now becomes two fold:

i). The point pattern of the simulated fractures must resemble the point pattern in Figure 3c in such a way that the point intensity field $\lambda(X)$ and the first and second moment measures, such as the inter-event distance function $H(t)$ and the K-function $K(t)$, are honoured (Stoyan et al. 1995).
ii). The simulated fractures must follow the mark distribution, the multivariate mark correlation and their spatial auto- and cross-mark correlations as described in 1 – 6 above.

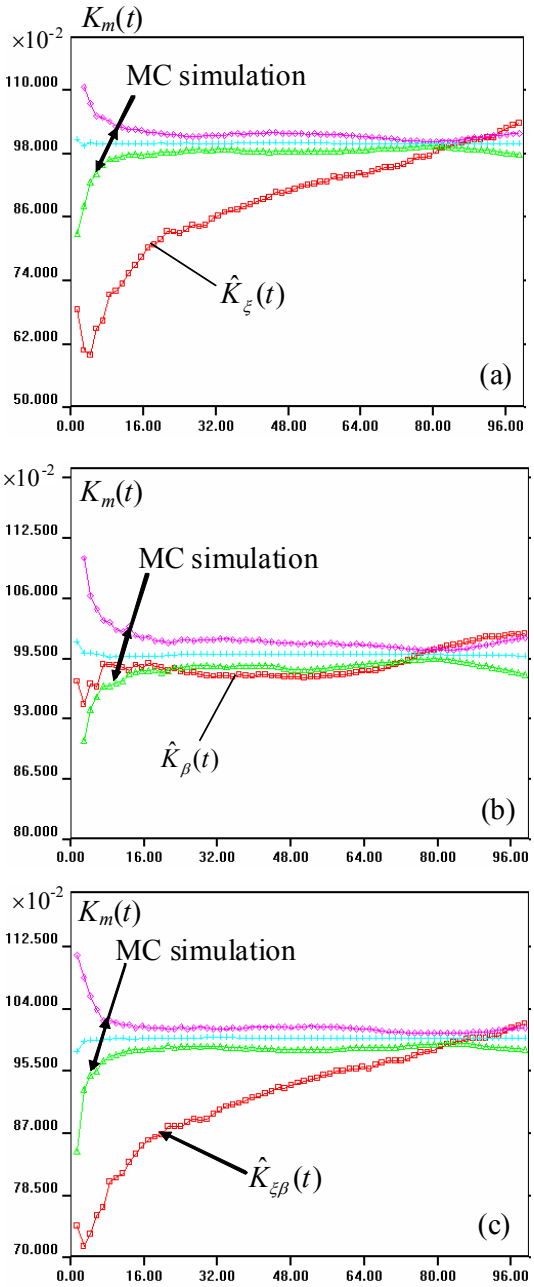

Figure 4 Corresponding cumulative mark correlation functions $\hat{K}_{\xi}(t)$ vs distance t (a), $\hat{K}_{\beta}(t)$ vs t (b) and $\hat{K}_{\xi\beta}(t)$ vs t (c) for the simulated example (Figure 3). The Monte Carlo (MC) simulation envelops shown are obtained for spatially uncorrelated marked point process

Problem i) can be solved, for example, by fitting an optimal non-parametric model (Xu et al., 2003). The second problem, however, cannot be easily resolved. Conditions 1 - 3 can be met by using a joint probability density function of ξ and β (α) for mark generation. We use simulated annealing to incorporate the spatial auto- and cross-correlation conditions (e.g., 4 - 6 above), as proposed in Xu et al. (2007).

Figure 5a shows a point realisation of the marked point process using a non-parametric model. This realisation is generated by a Boolean object

model and therefore initially the spatial auto- and cross-mark correlations of ξ, β and between ξ and β are non-existent. The realisation is then refined by simulated annealing and, after 1300 mark swaps, the final spatial mark correlation functions are given in Figure 6a and 6b, which indicate that the spatial mark correlation functions are closely reproduced at the end of the annealing process.

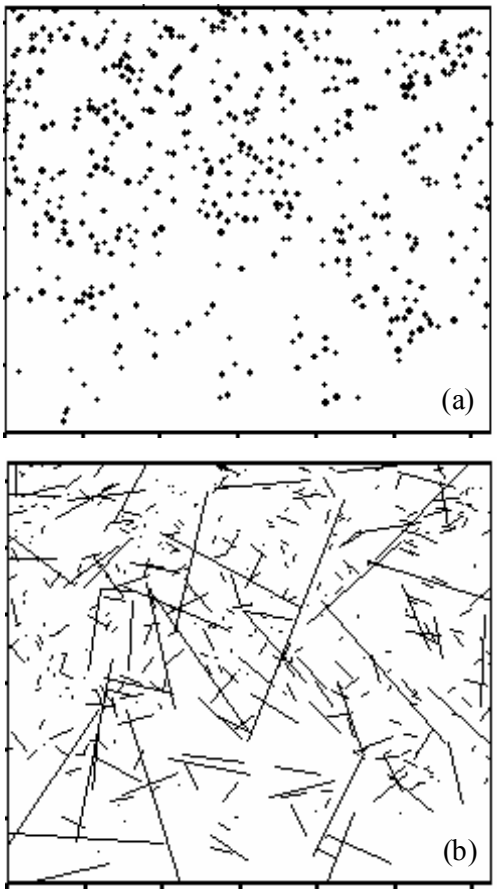

Figure 5 Simulated annealing process for the example shown in Figure 3 (a) One realisation from non-parametric model, (b) One realisation of the simulated fractures after annealing,

The final image of the simulated fractures, shown in Figure 5b, is not an exact replica of the original data (Figure 3b), but resembles the original data in the sense that the first and second moments of the characteristics of the corresponding marked point process (first and second order point intensity characteristics, mark distributions, multivariate mark correlations and spatial mark correlation functions) are reproduced.

Conclusions

Parameters of rock fractures (e.g., locations, orientation, size, aperture) are in generally spatially correlated. The correlations must be incorporated into the fracture model for realistic simulation of rock fracture system. The correlations can be quantified by cumulative spatial mark correlation function and the correlations can be effectively incorporated in the fracture model by simulation annealing.

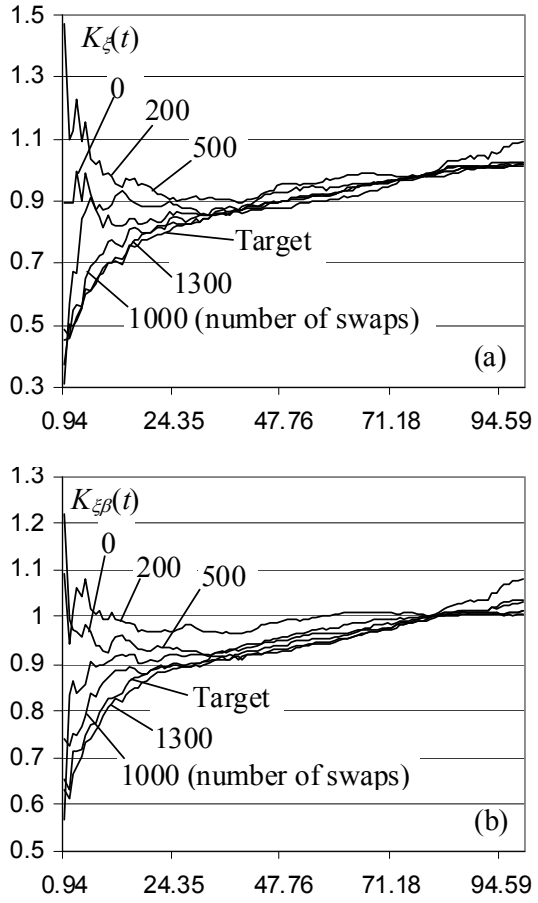

Figure 6 Simulated annealing process for the example shown in Figure 3 (a) $\hat{K}_\xi(t)$ vs distance *t*, (b) $\hat{K}_{\xi\beta}(t)$ vs *t*, (e)

References

Baghbanan, A. and Jing, L., 2007, Hydraulic properties of fractured rock masses with correlated fractures length and aperture, *International Journal of Rock Mechanics and Mining Science*, v. **44**, p. 704-719.

Barton, C.C. and Larson, E, 1985, Fractal geometry of two-dimensional fractures networks at Yucca Mountain, Southwest Nevada, proceedings of the International Symposium on Fundamentals of Rock Joints, O. Stephanson (ed.), Centek Publishers.

Chiles, J.P. & de Marsily G., 1993, Stochstic models of fracture systems and their use in flow and transport modelling, in *Flow and Contaminant Transport in Fractured Rock*, eds: Bear J., Tsang, C-F, and de Marsily, G., Academic Press.

Dershowitz, W. S. and Einstein, H. H., 1988, Characterizing rock joint geometry with joint system models, Rock Mechanics and Rock Engineering, v.**21**, p. 21-51.

Dowd, P. A., Xu, C., Mardia, K. V. and Fowell, R. J., 2007, A comparison of methods for the simulation of rock fractures, *Mathematical Geology*, v.**39**, p. 697 – 714.

Lee, C. H. & Farmer, I., 1993, *Fluid Flow in Discontinuous Rocks*, Chapman & Hall, London.

Lee, J. S., Veneziano, D., & Einstein, H. H., 1990, Hierarchical fracture trace model. Rock mechanics contributions and challenges, Proceedings of the 31th US Rock Mechanics Symposium, Hustrulid, W. & Johnson, G. A. (eds.), Balkema, Rotterdam.

Molchanov, I., 1997, Statistics *of the Boolean model for practitioners and mathematicians*, Wiley Series in Probability and Statistics, Wiley.

Priest, S. D., 1993, *Discontinuity Analysis for Rock Engineering*, Chapman & Hall, London.

Stoyan, D., Kendall, W. and Mecke, J., 1995, *Stochastic geometry and its applications*, 2nd edition, John Wiley & Sons, 436p.

Xu, C. and Dowd, P. A., 2009, A new computer code for discrete fracture network modelling, *Comps & Geosc.* (in press).

Xu, C. and Dowd, P. A., 2008, Plurigaussian simulation of rock fractures, *Proceedings of the Eight International Geostatistics Congress*, (eds. J.M. Ortiz and X. Emery), pub. Gecamin Ltd., ISBN 978-956-8504-17-5; v. **1**, p. 41-50.

Xu, C., Dowd, P. A., Mardia, K. V., Fowell, R. J. and Taylor, C. C., 2007, Simulating correlated marked point processes, *Journal of Applied Statistics*, v.**34**, 9, p. 1125 – 1134.

Xu, C., Dowd, P.A., Mardia, K.V. and Fowell, R., 2003, Stochastic approaches to fracture modelling. Internat. Assoc. for Mathematical Geology Conference, Sept., Portsmouth, UK